AGU PUBLICATIONS

Geophysical Research Letters

RESEARCH LETTER
10.1002/2016GL071313

Key Points:
- The article presents the first MLT Na retrievals from spaceborne Na D-line nightglow measurements
- The results confirm the overall validity of the Chapman Na D-line nightglow excitation mechanism
- Comparison of Na retrievals with independent observations allows constraining the branching ratio for the production of Na(2P) via NaO + O

Correspondence to:
C. von Savigny,
csavigny@physik.uni-greifswald.de

Citation:
von Savigny, C., M. P. Langowski, B. Zilker, J. P. Burrows, D. Fussen, and V. F. Sofieva (2016), First mesopause Na retrievals from satellite Na D-line nightglow observations, *Geophys. Res. Lett.*, *43*, 12,651–12,658, doi:10.1002/2016GL071313.

Received 22 SEP 2016
Accepted 21 NOV 2016
Accepted article online 25 NOV 2016
Published online 30 DEC 2016

First mesopause Na retrievals from satellite Na D-line nightglow observations

C. von Savigny[1], M. P. Langowski[1], B. Zilker[1], J. P. Burrows[2], D. Fussen[3], and V. F. Sofieva[4]

[1]Institute of Physics, Ernst-Moritz-Arndt-University of Greifswald, Greifswald, Germany, [2]Institute of Environmental Physics, University of Bremen, Bremen, Germany, [3]Belgian Institute for Space Aeronomy, Brussels, Belgium, [4]Finnish Meteorological Institute, Helsinki, Finland

Abstract We report the retrieval of Na concentration profiles in the mesopause region from satellite observations of the Na D-line nightglow emission near 589 nm made by the Scanning Imaging Absorption Spectrometer for Atmospheric Chartography (SCIAMACHY) on the Envisat spacecraft. The retrieval assumes the Na D-line excitation mechanism originally proposed by Chapman in 1939. The retrieval approach, including treatment of self-absorption by Na, a retrieval uncertainty budget, and first retrieval results, is presented. The retrieved Na profiles are compared to independent satellite measurements. Good agreement in terms of peak altitude, peak concentration, and vertical column density is found. The retrievals constitute the first Na profile retrievals from satellite observations of the Na D-line nightglow emission profile. They enable our understanding of the Na nightglow excitation mechanism to be tested.

1. Introduction

Na profile retrievals in the MLT (mesosphere/lower thermosphere) region typically use daytime satellite limb observations of sunlight resonantly scattered in the Na D-lines [e.g., *Gumbel et al.*, 2007; *Langowski et al.*, 2016], satellite stellar occultation measurements [*Fussen et al.*, 2010], or ground-based lidar observations [e.g., *She et al.*, 2000]. The Na D-lines also occur as an emission feature in the terrestrial nightglow spectrum [*Slipher*, 1929], and a first excitation mechanism for the Na D-line nightglow emission was proposed in 1939 by *Chapman* [1939]. This mechanism comprises the following reactions:

$$\mathrm{Na} + \mathrm{O_3} \xrightarrow{k_1} \mathrm{NaO} + \mathrm{O_2} \tag{1}$$

$$\mathrm{NaO} + \mathrm{O} \begin{cases} \xrightarrow{fk_2} \mathrm{Na}\left(^2\mathrm{P}_J\right) + \mathrm{O_2} \\ \xrightarrow{(1-f)k_2} \mathrm{Na}\left(^2\mathrm{S}_{1/2}\right) + \mathrm{O_2} \end{cases} \tag{2}$$

$$\mathrm{Na}\left(^2\mathrm{P}_J\right) \xrightarrow{A} \mathrm{Na}\left(^2\mathrm{S}_{1/2}\right) + h\nu \tag{3}$$

where k_1 and k_2 are reaction rate constants (units: $\mathrm{cm^3\ s^{-1}}$), $J = \{1/2, 3/2\}$ is the total angular momentum quantum number, f is the branching ratio for the production of $\mathrm{Na}(^2\mathrm{P}_J)$, and A is the Einstein coefficient (unit: s^{-1}) for spontaneous emission. Na retrievals from the Na D-line nightglow emission are of significance, because (a) the Na D-line nightglow excitation mechanism is not fully understood [e.g., *Plane et al.*, 2015] and (b) measurements of Na in the MLT region are needed to constrain quantitatively the daily meteoric mass influx, which is still highly uncertain [e.g., *Plane*, 2012]. The main objective of the present study is to present an Na retrieval based on the Na D-line nightglow emission as well as first comparisons of this data product with independent measurements. It is planned in the future to use the new Na data product to investigate our understanding of the excitation mechanism of the Na D-line nightglow emission.

2. Instruments and Data

The Na D-line nightglow measurements used in this study were performed with SCIAMACHY, the Scanning Imaging Absorption Spectrometer for Atmospheric Chartography on ESA's (European Space Agency) Envisat

spacecraft [*Burrows et al.*, 1995]. SCIAMACHY was a grating spectrometer that carried out spectroscopic measurements in nadir, occultation, and limb viewing geometry from August 2002 to April 2012. SCIAMACHY made observations in the 220 nm to 2380 nm spectral range in eight spectral channels—contiguously between 220 and 1750 nm (channels 1–6), between 1940 and 2040 nm (channel 7), and between 2265 and 2380 nm (channel 8)—with a wavelength-dependent spectral resolution between 0.2 and 1.5 nm. Around 589 nm—the wavelength relevant here—SCIAMACHY spectra are measured with about 0.2 nm spectral sampling and a sampling ratio of about 2. For this study only the mesosphere/lower thermosphere limb measurements on the Earth's nightside were used. Envisat flies in a heliosynchronous orbit with a 10:00 A.M. descending node. Consequently, the low-latitude nighttime measurements presented here were made at around 10:00 P.M. local solar time.

The O_3 concentration profiles required for the derivation of Na profiles were retrieved using measurements by the GOMOS (Global Ozone Measurements by Occultation of Stars) instrument [*Bertaux et al.*, 2010], also aboard Envisat. GOMOS performed highly accurate O_3 measurements up to about 105 km altitude during nighttime [e.g., *Kyrölä et al.*, 2010], and the observations were carried out at a local solar time close to the one of the SCIAMACHY nighttime limb observations used here.

3. Methodology

Xu et al. [2005] presented a theoretical approach to retrieve MLT Na profiles from observations of vertical volume emission rate profiles of the Na D-line nightglow at 589 nm. One important result of this study was that the complex Na chemistry is dominated by three reactions, i.e., reactions (1) and (2) of the Chapman mechanism and the following additional Na loss reaction:

$$\mathrm{Na} + \mathrm{O_2} + M \xrightarrow{k_3} \mathrm{NaO_2} + M \tag{4}$$

As demonstrated by *Xu et al.* [2005], ignoring all other neutral, ionic, or photochemical reactions leads to Na retrieval uncertainties of less than 1% in the 85–110 km altitude range, where almost all of the MLT Na resides. Assuming (a) that a steady state is achieved by reactions (1), (2), and (4); (b) that the sum of [Na(^{2}P)] and [Na(^{2}S)] is in steady state; and (c) considering that quenching of Na(^{2}P) is negligible leads to the following relationship between the Na nightglow volume emission rate (VER in photons s^{-1} cm^{-3} with VER = [Na(^{2}P)] × A) and Na concentration $[\mathrm{Na}]_{\mathrm{ret}}$:

$$[\mathrm{Na}]_{\mathrm{ret}} = \frac{\mathrm{VER}/f}{k_1\left[\mathrm{O_3}\right] + k_3\left[\mathrm{O_2}\right][M]}\,. \tag{5}$$

This model is used in the current study to retrieve Na concentration profiles from SCIAMACHY Na D-line nightglow observations. The retrieval uses the Na D-line VER profiles from SCIAMACHY nighttime limb observations and the above equation to infer Na density profiles. Na D-line VER profiles are retrieved from SCIAMACHY nighttime observations of the limb emission rate (LER) profile measurements using the constrained linear least squares approach described in detail by *von Savigny et al.* [2012].

An important aspect of this method is the remaining uncertainty of the branching ratio f. The published values for f span a considerable range from <0.01 [*Plane and Husain*, 1986] up to 2/3 [*Herschbach et al.*, 1992]. The reasons for these relatively large differences are partly understood [e.g., *Plane et al.*, 2015] and are related to the different electronic states of NaO, i.e., NaO($A^2\Sigma$) and NaO($X^2\Pi$) relevant for reactions (1) and (2). *Clemesha et al.* [1995] found an optimum value of $f = 0.093$ by searching for the best agreement between modeled and an observed Na density profile. For the initial Na retrieval results presented here we assume a value of $f = 0.09$, based on the results by *Clemesha et al.* [1995]. In a future study we will attempt constraining the value of f based on comparisons of our retrievals with ground-based lidar and other satellite observations that are not based on the Na D-line nightglow emission.

Retrieving Na density profiles using equation (5) also requires knowledge of several other parameters and rate constants. The O_3 concentration profiles are taken from a monthly averaged O_3 concentration climatology—as a function of geometric altitude—based on GOMOS stellar occultation observations. The O_2, N_2, and temperature profiles were taken from the NRL-MSISE-00 model. The reaction rate constants $k_1 = 1.1\times10^{-9}\exp(-116/T)$ cm^3 s^{-1} and $k_3 = (5.0\times10^{-30})(T/200)^{-1.22}$ cm^6 s^{-1} were taken from *Plane et al.* [2015].

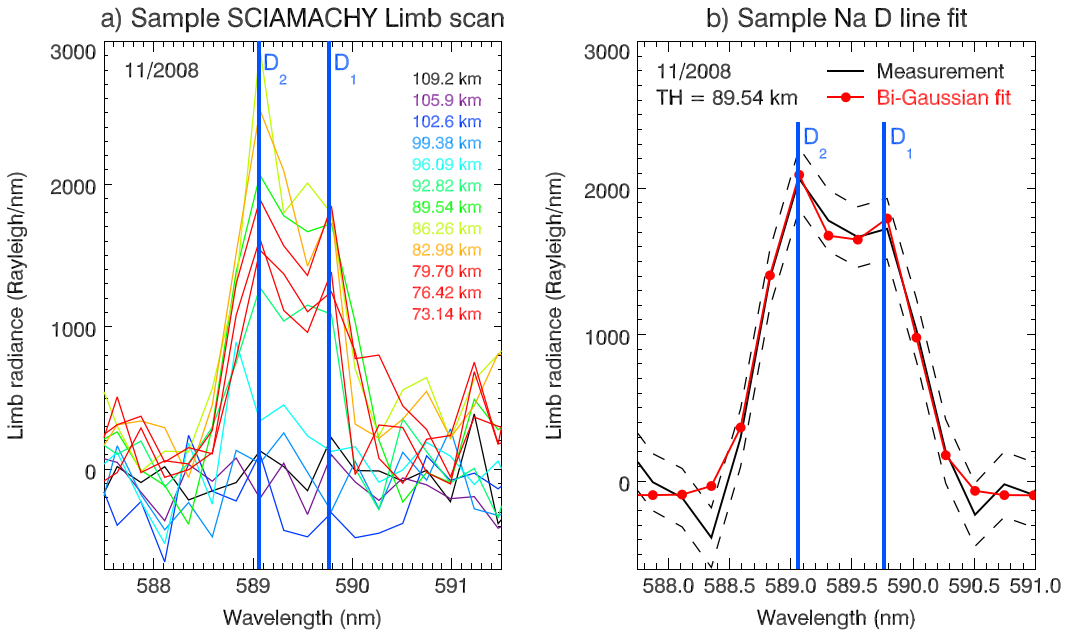

Figure 1. (a) Sample monthly averaged Na D-line emission spectra at different tangent heights for November 2008 and the 30°S–30°N latitude range. (b) Sample monthly averaged Na D-line emission spectrum (black line) with bi-Gaussian fit (red line and circles) for November 2008 and about 89.5 km tangent height. The black dashed lines correspond to the random errors of the limb radiance measurements.

3.1. Retrieval Approach and Self-Absorption Correction

The signal-to-noise ratio (SNR) of the SCIAMACHY nighttime limb spectra is such that the retrieval of Na profiles is not possible for individual limb observations. Even for zonally and daily averaged measurements the SNR is insufficient. For this reason, the Na profile retrieval is currently based on monthly averaged limb spectra. In addition, all limb measurements in the 30°S to 30°N latitude range were averaged. All retrievals use SCIAMACHY level 1c data version 7.0x calibrated with the `scialc` tool [*Deutsches Zentrum für Luft- und Raumfahrt*, 2015] with all calibration flags applied. Orbital data affected by instrumental or platform anomalies were screened the same way as in the case of the MLT atomic oxygen profile retrievals from SCIAMACHY oxygen green line observations described by *Lednyts'kyy et al.* [2015].

Figure 1a shows monthly averaged Na D-line emission spectra for November 2008 and different tangent heights. Note that for observations at a given tangent height the line of sight passes through atmospheric layers at elevated altitudes. The emission from these layers accounts for the observation of Na emission at the lower altitudes, e.g., at 73 km, where the retrieved Na concentration is negligible within error. The limb emission rates (LER) are determined by fitting a combination of a constant offset, a linear component, and two Gaussian functions to the emission spectrum at each tangent height. The two Gaussians represent the atmospheric Na D-line emission, while the constant and linear components correspond to potential instrumental effects. Figure 1b shows a sample fit to a monthly averaged emission spectrum for November 2008 at about 89.5 km tangent height.

The self-absorption of the Na D-line emission by Na in the mesopause region cannot be neglected. A self-absorption correction identical to the one applied to Na profile retrievals from SCIAMACHY daytime limb observations of resonantly scattered solar radiation (see *Langowski et al.* [2016] for a detailed description) has been implemented. Note that the excitation of the Na D-line dayglow emission is based on a completely different mechanism, i.e., resonance flourescence, compared to the chemiluminescent excitation of the nightglow emission. However, the treatment of self-absorption by Na is the same in both cases. For typical Na density profiles with vertical column densities of about 3×10^9 cm^{-2} the line of sight optical depth from the tangent point to the instrument and associated with self-absorption by Na is about 0.5. Note that this is consistent with the differences in VER (and also Na) profiles between the first and the final iterations (see Figure 3). The self-absorption correction requires an iterative retrieval. The Na profiles are not a direct outcome of the inversion procedure; rather, the inferred VER profiles are converted to Na density profiles using the photochemical

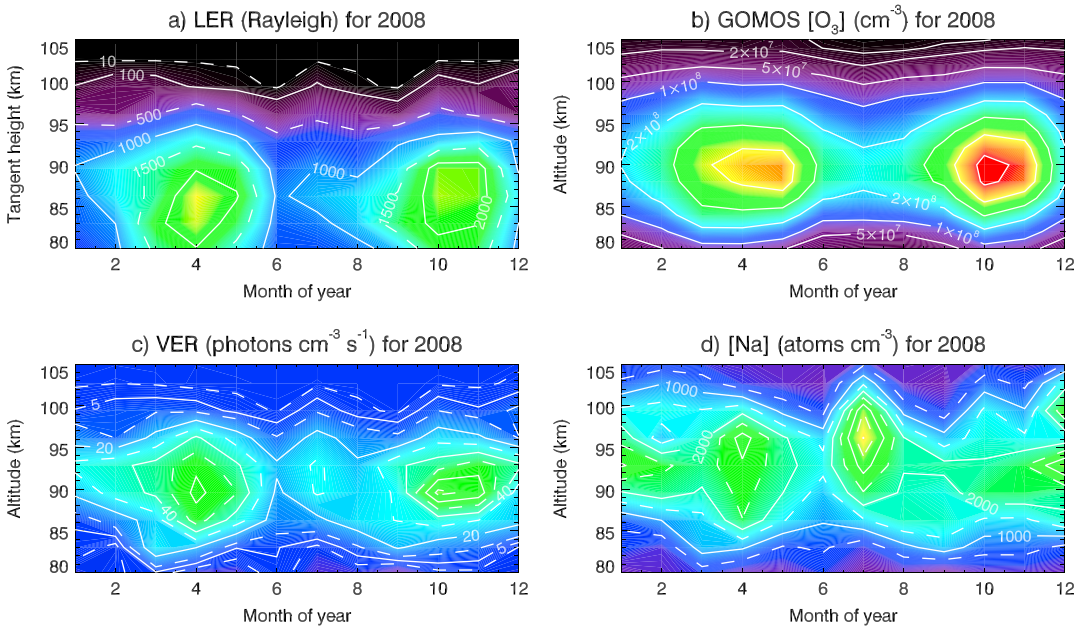

Figure 2. (a) Na D-line limb emission rate (LER) in Rayleigh (1R = 10^6 photons s^{-1} cm^{-2}) as a function of time and tangent height for 2008. (b) Time and altitude dependence of monthly averaged O_3 densities retrieved from GOMOS stellar occultation observations. The retrieved (c) volume emission rate (VER) and (d) Na density fields as a function of time and altitude for 2008 with self-absorption correction and a branching ratio of $f = 0.09$. The data in all panels were averaged over the 30°S to 30°N latitude range.

model described above. In the first iteration self-absorption is neglected and a first estimate of the VER and subsequently Na density profile is retrieved. In the standard setup 10 iterations of the retrievals are performed, but the retrieval results typically change by less than 1% after the fifth iteration. Due to the nonlinearity of the self-absorption correction, it is in principle possible that the retrieval diverges. However, diverging retrievals have not occurred.

Figure 2a shows the time and tangent height variation of the observed LER profiles (in Rayleigh) for the year 2008 and averaged over the 30°S–30°N latitude range. Figure 2b shows the variation of monthly averaged GOMOS ozone concentrations for the same year. Figures 2a and 2b show clear evidence of the well-known semiannual variation at low latitudes.

3.2. Sample Retrieval Results

Figure 3 shows sample retrieval results for November 2008 and a branching ratio of $f = 0.09$. Figure 3a displays the inverted VER profiles for the first (black) and the following iterations. The final (i.e., tenth) iteration is shown in red. The dashed lines represent the propagated uncertainty and are only shown for the final iteration. The LER uncertainties used for this purpose correspond to the standard errors of the mean of the monthly averaged LER profiles. The LER profile and its uncertainties for November 2008 are shown in black in Figure 3c. The red line in Figure 3c corresponds to the reconstructed or forward modeled LER profile based on the Na density profile from the last iteration step. The fact that the observed LER profile is well reproduced by the retrieval constitutes an important consistency check. Figure 3b shows the retrieved Na density profiles after the first (black) and the following iterations. The blue dashed line displays a Gaussian fit to the final iteration; it peaks at 91.7 km and has a full width at half maximum (FWHM) of 12.3 km. The peak altitude and the peak density (2000–2500 atoms cm^{-3}) are in good agreement with independent observations, as further discussed below in section 3.4.

Figures 2c and 2d show the retrieved time and altitude variations in VER and Na concentration, respectively, for the year 2008 and $f = 0.09$. The semiannual variation clearly present in LER, O_3, and VER is not that pronounced in the Na retrievals, in qualitative agreement with the SCIAMACHY daytime Na retrievals presented

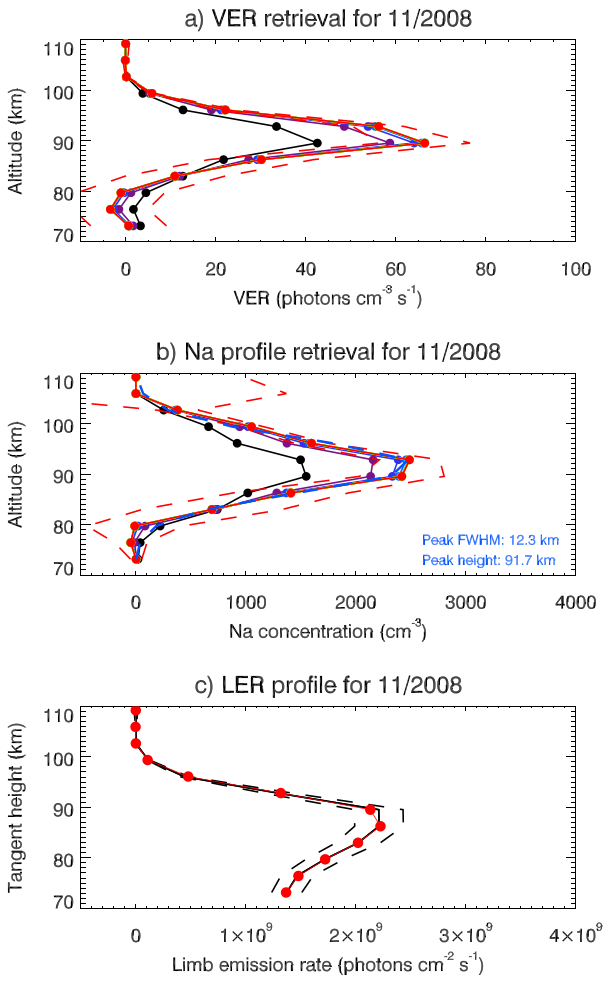

Figure 3. Sample iterative retrieval of (a) Na D-line VER and (b) Na density profiles for November 2008 and a branching ratio of $f = 0.09$. The black, violet, blue, and red lines show the results of the first, second, third, and tenth iterations. The dashed lines correspond to the propagated errors of the mean of the integrated limb emission rates (only shown for the tenth iteration). (c) The black solid line shows the observed limb emission rate (LER) profile—spectrally integrated over both the D_1 and D_2 lines. The dashed black lines correspond to the standard error of the mean of the monthly averaged LER profiles. The red line shows the forward modeled LER profile based on the last iteration of the Na profile retrieval.

by *Langowski et al.* [2016]. Figure 2 suggests that the semiannual variation in the Na D-line emission is mainly caused by a semiannual variation in O_3 and to a lesser degree by a semiannual variation in Na itself.

3.3. Retrieval Uncertainties

We now briefly discuss possible sources of uncertainty for the Na profile retrieval. We distinguish between random errors and parameter errors—the latter being caused by incorrect knowledge of parameters affecting the Na profile retrievals, i.e., $[O_3]$, $[O_2]$, $[N_2]$, and temperature; the rate constants k_1 and k_3; and the value of the branching ratio f. Table 1 provides an overview of the sources of uncertainty considered. The random Na retrieval uncertainties listed in Table 1 correspond to the propagated errors of the mean of the monthly averaged LER profiles. We note that these uncertainties include both natural variability of LER profiles about the monthly mean and measurement noise. The parameter errors are determined by repeating the Na profile retrievals with perturbed parameters, followed by calculating relative differences with respect to the reference retrievals. The temperature profile was perturbed by 10 K, O_3 concentration was perturbed by 5%—corresponding to the uncertainty of the GOMOS O_3 in the MLT region—and neutral density, and the reaction rates k_1 and k_3 were perturbed by 10%. The branching ratio f was altered from the nominal value ($f = 0.09$) to $f = 0.1$. An uncertainty in f of 0.01 appears small in view of the large range of published branching ratio values. However, changing f by ± 0.01 leads to peak-to-peak variations in Na vertical column density of about 40%. When f is changed by ± 0.02, then the peak-to-peak changes in Na vertical column density reach almost 100%. This nonlinear behavior is caused by the self-absorption of the Na D-line emission by Na. Given the high sensitivity of the Na retrievals to the value of f (see also section 3.4), an uncertainty of ± 0.01 is a reasonable assumption. The determination of uncertainties was carried out for all months of the year 2008, and the uncertainties were then averaged annually.

Determination of a total uncertainty is essentially impossible in a strict mathematical sense. Simply adding the individual relative uncertainties would lead to an overestimation of the actual retrieval uncertainties. The approach taken is that the variances of the individual uncertainty contributions are added to yield the total variance. The obtained total uncertainty estimate is shown in the last row of Table 1 and amounts to 30–40% for the 90–100 km altitude range. One of the largest uncertainty contributions is due to the uncertainty in f—as expected. Below and above the Na density peak random uncertainties dominate. Improvement in the

Table 1. Overview of Sensitivity Study Results for the Na Profile Retrieval

Parameter	Perturbation	85 km	90 km	95 km	100 km
Branching ratio *f*	+0.01	−11.7%	−15.6%	−16.4%	−15.3%
Temperature	+10 K	−0.7%	−4.3%	−5.0%	−4.5%
Ozone	+5%	−4.4%	−7.4%	−8.0%	−7.4%
Neutral density	+10%	−5.2%	−1.4%	−0.7%	−0.4%
Random uncertainty	not applicable	50.5%	17.0%	10.5%	27.7%
k_1	+10%	−8.3%	−13.8%	−14.7%	−13.8%
k_3	+10%	−2.6%	−0.7%	−0.4%	−0.2%
Total uncertainty	not applicable	53.0%	28.3%	26.2%	35.6%

knowledge of the branching ratio *f* from laboratory studies will reduce the uncertainty on the determination of Na concentration using this method.

3.4. Comparison to Independent Results

We now compare the retrieved Na density profiles and vertical column densities to independent observations. Figure 4a shows a comparison of Na vertical column density (VCD)—i.e., the vertically integrated Na density profile—derived from the SCIAMACHY nighttime observations with VCDs obtained from GOMOS

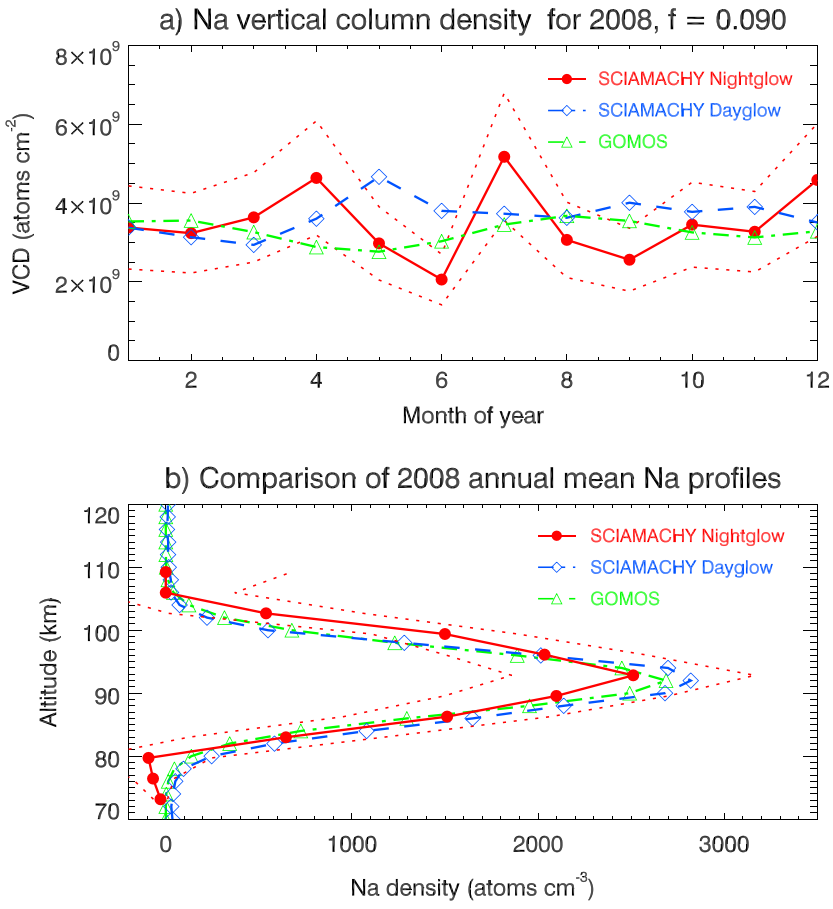

Figure 4. (a) Comparison of monthly averaged Na vertical column density (VCD) for 2008 retrieved from SCIAMACHY nightglow observations ($f = 0.09$; red solid line) with retrievals based on SCIAMACHY dayglow observations (blue dashed line) and GOMOS stellar occultations (green dash-dotted line). (b) Comparison of annually averaged Na density profiles retrieved from SCIAMACHY nightglow and dayglow measurements as well as GOMOS observations (same line/color convention as in Figure 4a). The red dotted lines in the two panels correspond to the total retrieval uncertainties presented in Table 1.

stellar occultation observations [*Fussen et al.*, 2010], as well as from SCIAMACHY resonance fluorescence observations on the Earth's dayside [*Langowski et al.*, 2016]. The independent data sets were averaged over the 30°S–30°N latitude range. The SCIAMACHY daytime values represent multiannual mean seasonal variations for the years 2008–2012, as described in *Langowski et al.* [2016]. The relative difference in annually averaged Na VCD between the SCIAMACHY nightglow and the independent reference data sets, i.e., $\left([\mathrm{Na}]_{\mathrm{Nightglow}} - [\mathrm{Na}]_{\mathrm{ref}}\right) / [\mathrm{Na}]_{\mathrm{ref}}$, is −4.6% for the SCIAMACHY daytime retrievals and +6.7% for the GOMOS retrievals for a branching ratio of $f = 0.09$. If the branching ratio is chosen to be $f = 0.10$, then the relative difference to the SCIAMACHY daytime retrievals is −18.6% and the difference to the GOMOS observations is −8.9%. We found that $f = 0.09$ yielded the best agreement of VCDs with the GOMOS and SCIAMACHY daytime observations, when changing f in steps of 0.01. The SCIAMACHY nighttime Na retrievals exhibit more variability than the GOMOS and the SCIAMACHY daytime retrievals, which is likely related to the poorer SNR of the nightglow emission measurements.

Figure 4b shows a comparison of annually averaged Na density profiles based on SCIAMACHY nightglow (with $f = 0.09$), SCIAMACHY dayglow, and GOMOS stellar occultation observations. The maximum Na density of the SCIAMACHY nightglow profile is lower than for the other two profiles, while its peak is slightly wider than for the other two profiles. The reasons for these differences are currently not fully understood. However, the overall agreement between the different profiles can be considered good. In a future and more comprehensive study the SCIAMACHY nightglow Na retrievals will be compared systematically to independent observations with the goal of establishing an optimal value of the branching ratio f.

4. Conclusions

We reported on the first Na profile retrievals in the mesopause region from satellite Na D-line nightglow profile observations. The retrieval is based on the Na D-line excitation mechanism initially proposed by Chapman in 1939. One major source of uncertainty is the inaccurate knowledge of the branching ratio f of the reaction between O and NaO. Choosing $f = 0.09$ — in good agreement with earlier ground-based observations — we find good agreement in terms of vertical Na columns and profiles with independent satellite observations. Our results provide a unique data set for testing the Na D-line nightglow excitation mechanism, which is still not fully understood.

Acknowledgments
This work was supported in part by the European Space Agency (ESA) through project MesosphEO, Ernst-Moritz-Arndt-University of Greifswald, the German Aerospace Center (DLR), and the University of Bremen. We thank the European Space Agency for providing SCIAMACHY Level 1 data. The SCIAMACHY Level 1 data used in this study are accessible through an ESA web interface (https://earth.esa.int/web/guest/home).

References

Bertaux, J.-L., et al. (2010), Global ozone monitoring by occultation of stars: An overview of GOMOS measurements on ENVISAT, *Atmos. Chem. Phys.*, *10*(24), 12,091–12,148, doi:10.5194/acp-10-12091-2010.

Burrows, J. P., E. Hölzle, A. P. H. Goede, H. Visser, and W. Fricke (1995), SCIAMACHY — Scanning Imaging Absorption Spectrometer for Atmospheric Chartography, *Acta Astronaut.*, *35*(7), 445–451.

Chapman, S. (1939), Notes on atmospheric sodium, *Astrophys. J.*, *90*, 309–316.

Clemesha, B. R., D. M. Simonich, H. Takahashi, S. M. L. Melo, and J. M. C. Plane (1995), Experimental evidence for photochemical control of the atmospheric sodium layer, *J. Geophys. Res.*, *100*, 18,909–18,916.

Deutsches Zentrum für Luft- und Raumfahrt (2015), SCIAMACHY Command Line Tool Software user's manual (SUM), SCIAMACHY Level 1b to 1c processing, DLR technial report, ENV-SUM-DLR-SCIA-0071, Issue 3C. [Available at https://earth.esa.int/documents/10174/2481822/SciaL1c-Command-line-Tool-Software-User-Manual.]

Fussen, D., et al. (2010), A global climatology of the mesospheric sodium layer from GOMOS data during the 2002–2008 period, *Atmos. Chem. Phys.*, *10*, 9225–9236, doi:10.5194/acp-10-9225-2010.

Gumbel, J., Z. Y. Fan, T. Waldemarsson, J. Stegman, G. Witt, E. Llewellyn, C.-Y. She, and J. M. C. Plane (2007), Retrieval of global mesospheric sodium densities from the Odin satellite, *Geophys. Res. Lett.*, *34*, L04813, doi:10.1029/2006GL028687.

Herschbach, D. R., C. E. Kolb, D. R. Worsnop, and X. Shi (1992), Excitation mechanism of the mesospheric sodium nightglow, *Nature*, *356*, 414–416.

Kyrölä, E., et al. (2010), Retrieval of atmospheric parameters from GOMOS data, *Atmos. Chem. Phys.*, *10*, 11,881–11,903, doi:10.5194/acp-10-11881-2010.

Langowski, M. P., C. von Savigny, J. P. Burrows, V. V. Rozanov, T. Dunker, U.-P. Hoppe, M. Sinnhuber, and A. C. Aikin (2016), Retrieval of sodium profiles in the mesosphere and lower thermosphere from SCIAMACHY limb emission measurements, *Atmos. Meas. Tech.*, *9*, 295–311.

Lednyts'kyy, O., C. von Savigny, K.-U. Eichmann, and M. G. Mlynczak (2015), Atomic oxygen retrievals in the MLT region from SCIAMACHY nightglow limb measurements, *Atmos. Meas. Tech.*, *8*, 1021–1041, doi:10.5194/amt-8-1021-2015.

Plane, J. M. C. (2012), Cosmic dust in the Earth's atmosphere, *Chem. Soc. Rev.*, *41*, 6507–6518.

Plane, J. M. C., and D. Husain (1986), Determination of the absolute rate constant for the reaction O + NaO ⟶ Na + O_2 by time-resolved atomic chemiluminescence at λ = 589 nm ($Na(3^2P_J) \rightarrow Na(3^2S_{1/2}) + h\nu$), *J. Chem. Soc. Faraday Trans.*, *2*(82), 2047–2052.

Plane, J. M. C., W. Feng, and E. C. M. Dawkins (2015), The mesosphere and metals: Chemistry and changes, *Chem. Rev.*, *115*, 4497–4541, doi:10.1021/cr500501m.

She, C. Y., S. Chen, Z. Hu, J. Sherman, J. D. Vance, V. Vasoli, M. A. White, J. Yu, and D. A. Krueger (2000), Eight-year climatology of nocturnal temperature and sodium density in the mesopause region (80 to 105 km) over Fort Collins, CO (41°N, 105°W), *Geophys. Res. Lett.*, *27*, 3289–3292.

Slipher, V. M. (1929), Emissions in the spectrum of the light of the night sky, *Publ. Astron. Soc. Pac.*, *41*, 262–263.

von Savigny, C., I. C. McDade, K.-U. Eichmann, and J. P. Burrows (2012), On the dependence of the OH* Meinel emission altitude on vibrational level: SCIAMACHY observations and model simulations, *Atmos. Chem. Phys.*, *12*, 8813–8828, doi:10.5194/acp-12-8813-2012.

Xu, J., A. K. Smith, and Q. Wu (2005), A retrieval algorithm for satellite remote sensing of the nighttime global distribution of the sodium layer, *J. Atmos. Sol. Terr. Phys.*, *67*, 739–748.